BMC Endocrine Disorders

RESEARCH

Open Access

Associations between pathological features and radioactive iodine-refractory recurrent papillary thyroid carcinoma: with mutation analysis using recurrent samples

Thi Nhung Nguyen[1†], Zhanna Mussazhanova[1,2†], Hirokazu Kurohama[1], Van Dong Hoang[3], Ngoc Ha Le[4], Thi Minh Hanh Ngo[5], Van Phu Thang Nguyen[1], Katsuya Matsuda[1], Yuki Matsuoka[1], Katsiaryna Tratsiakova[1], Thi Ngoc Anh Nguyen[1], Yerkezhan Sailaubekova[1], Thi Phuong Nguyen[4], Minh Son Le[5] and Masahiro Nakashima[1*]

Abstract

Background Although papillary thyroid carcinomas (PTC) are usually indolent in nature and clinically controllable, two-thirds of metastatic diseases become radioactive iodine-refractory (RAI-R). This study aimed to determine the role of pathological features, *BRAF*^{V600E}, *TERT* promoter (*TERT*-p), and their combinations on Vietnamese patients with RAI-R recurrent PTC.

Methods This cross-sectional study included 174 cases of locoregional recurrent PTC, including 135 and 39 RAI-R and RAI-avid (RAI-A) cases, respectively. Logistic regression analyses were used to evaluate the associations between pathological features, mutations, and RAI-R with tissues from recurrent lesions.

Results Loss of polarity/loss of cell cohesiveness (LOP/LCC) component was exclusively observed in recurrent cancers in the RAI-R group. RAI-R was associated with *BRAF*^{V600E} mutation, *TERT*-p mutation, *BRAF*^{V600E}/*TERT*-p single mutant (Smut), *BRAF*^{V600E}/*TERT*-p double mutant (Dmut), tall cell component, and mitosis ≥ 2/2 mm^2 in the unadjusted logistic regression analysis. Multivariable logistic regression analysis revealed that *BRAF*^{V600E} mutation and Dmut were independent predictors of RAI-R. The presence of Dmut (odds ratio [OR] = 6.64) was more significantly associated with RAI-R compared with that of Smut (OR = 2.75). There was a marginal association between tall cell > 5%, mitosis count ≥ 2/2 mm^2 and RAI-R. The combination of *BRAF*^{V600E}/tall cell components was the strongest predictor of RAI-R.

Conclusions RAI-R PTC cases were independently associated with *BRAF*^{V600E}, Dmut. The association between Dmut and RAI-R PTC was stronger than that between Smut and RAI-R PTC. Future studies should focus on elucidating the role of mitotic count and LOP/LCC in RAI-R PTC.

†Thi Nhung Nguyen, Zhanna Mussazhanova these authors contributed equally to this study.

*Correspondence:
Masahiro Nakashima
moemoe@nagasaki-u.ac.jp

Full list of author information is available at the end of the article

Keywords Radioactive iodine refractory, Recurrent papillary thyroid carcinoma, *BRAF*^{V600E}, *TERT* promoter, Tall cell, Mitosis

Introduction

Papillary thyroid carcinoma (PTC) is the most prevalent histological subtype of thyroid cancer, accounting for 90% of all thyroid carcinomas [1]. Generally, thyroid cancer has a favorable prognosis, with 80–95% of thyroid carcinomas achieving an overall survival rate of 10 years [2]. Nevertheless, local recurrence and distant metastases account for 20% and 15% of all cases, respectively [2]. Additionally, two-thirds of metastatic diseases become refractory to radioactive iodine (RAI) at the initial diagnosis or gradually during follow-up [3]. In cases of differentiated thyroid cancer with distant metastasis, although the 10-year survival rate was > 50% in RAI-avid (RAI-A) patients, it was only 10% in RAI-refractory (RAI-R) patients [3]. Locoregional recurrent PTCs are usually treated by reoperation, followed by additional RAI therapy with complementary thyroid resection [4]. In cases of RAI-R with progressive disease and multiple lesions, tyrosine kinase inhibitors (e.g., sorafenib, lenvatinib) can be indicated [5]. Therefore, previous studies have attempted to clarify the clinicopathological features associated with RAI-R, which provide additional insights for improving prognosis and management strategies [6–8].

Coexisting *BRAF*^{V600E} and Telomere Reverse Transcriptase promoter (*TERT*-p) mutations robustly affect RAI-R [9, 10]. However, the role of *BRAF*^{V600E} on RAI-R was controversial [8–14] and is yet to be elucidated. Previous studies also found a significant association between aggressive histological subtypes of PTC, such as tall cell and hobnail, and an increased risk of RAI-R [6, 8]. Additionally, recent studies have suggested that even focal tall cell change, with height of cells at least three times their width and their rate < 30% of tumor areas, should be reported at any proportion because of its worse prognosis than those without any tall cells [15, 16]. Loss of polarity/loss of cell cohesiveness (LOP/LCC) components, such as hobnail and micropapillary structures, in the invasive front have been identified as a valuable morphological indicator of epithelial-mesenchymal transition (EMT) in PTC, related to a higher rate of recurrence/metastases and cancer-related death [17, 18]. However, little was known about whether focal tall cell change and LOP/LCC are related to RAI-R. In terms of mitosis count and Ki-67 labeling index (LI), which were well described in association with recurrence and mortality of PTC [19–21], roles of these features remain to be investigated for RAI-R.

Therefore, this study evaluated the association between RAI-R and histopathologic characteristics, including the ratio of aggressive features of PTC, such as tall cell and LOP/LCC components, mitosis count, and Ki-67 LI. Furthermore, this study firstly describes the association between coexisting clinicopathological features with mutation status on the risk of RAI-R in our recurrent PTC cohort from Vietnamese patients.

Materials and methods

Study setting and participants

This cross-sectional study included patients who underwent reoperation for locoregional recurrence between September 2020 and June 2023 at 108 Military Central Hospital in Hanoi, Vietnam. A total of 193 patients with PTC were initially eligible, of which 174 met the following inclusion criteria: (i) aged ≥ 19 years at initial diagnosis; (ii) total thyroidectomy followed by RAI treatments at the time of initial surgery for PTC; (iii) no history of other cancers; (iv) recurrence defined as thyroid bed or regional lymph node lesions occurring in patients clinically disease-free for 6 months after total thyroidectomy [22, 23]; and (v) sufficient tissue specimens from surgically resected cases for molecular and histological analysis. Patients were classified into two groups, RAI-A and RAI-R, according to the presence or absence of RAI avidity of recurrent tumors on post-therapeutic and/or ^{131}I diagnostic whole-body scans, with appropriate TSH stimulation and iodine preparation. RAI-A was defined as RAI uptake in all known recurrent lesions. RAI-R was defined as the loss of RAI avidity, where one or more lesions show no RAI uptake [9]. This definition includes recurrent/metastatic lesions that do not concentrate RAI or concentrate RAI in some lesions but not in others [4]. To ensure accurate RAI scans, patients followed a low-iodine diet for two weeks and underwent thyroid hormone withdrawal for four weeks (or two weeks if using triiodothyronine for the preceding two weeks) to elevate the thyroid-stimulating hormone level of ≥ 30 μIU/mL.

Histological and mutation analyses

Histological and mutation analyses were conducted at the Department of Tumor and Diagnostic Pathology, Atomic Bomb Disease Institute, Nagasaki University, Nagasaki, Japan. Information about *BRAF*^{V600E}, *TERT*-p mutations, tall cell components, LOP/LCC components in the invasive front, mitosis count/2 mm^2, and Ki-67 LI was obtained from 174 formalin-fixed paraffin-embedded (FFPE) samples, including 156 cases (89.7%) from lymph nodes and 18 cases (10.3%) from thyroid beds. All these samples were recurrent/metastasis tissues obtained from reoperations for recurrence disease, with a median time

from total thyroidectomy to reoperation of 41.8 months (8.1–199.5 months).

To analyze $BRAF^{V600E}$ and *TERT*-p mutations, we extracted genomic DNA from tumor areas in the FFPE tissue samples. Tumor areas, identified using a guide slide stained with hematoxylin and eosin (H&E), were macrodissected from each 8-µm-thick section. A Maxwell RSC DNA FFPE Kit (Promega) was used for genomic DNA extraction according to the manufacturer's instructions. We used a NanoDrop-1000 spectrophotometer to quantify the extracted DNA. $BRAF^{V600E}$ and *TERT*-p (C228T and C250T) were detected using primer/probe sets (Bio-Rad) and droplet digital polymerase chain reaction according to previously described protocols [24–26]. We classified the mutation status into the following three groups: wild-type, $BRAF^{V600E}$/*TERT*-p mutation only (single mutant: Smut), and coexistence of $BRAF^{V600E}$ and *TERT*-p mutations (double mutant: Dmut) to evaluate the role of each mutation status and their combination with other pathological features, such as Ki-67 LI, mitosis count, and presence of tall cell components (> 5%).

Ki-67 immunostaining was performed using a primary anti-Ki-67 antibody (clone MIB1; Monoclonal Mouse, Dako, Glostrup, Denmark). Staining was performed using a Ventana Benchmark Autostainer (Roche, Indianapolis, IN, USA). To evaluate Ki-67 expression, we quantified the number of positively stained cells at ×400 in the identified hotspot regions, as previously reported [27]. Staining results were categorized into two groups, ≤ 3% and > 3%, according to findings from previous studies [19, 20]. Two pathologists (Z.M. and H.K.) independently reviewed the tumor samples. In cases of disagreement, the pathologists conducted a joint reassessment to ensure consistent evaluation of Ki-67 LI.

Histopathologic diagnoses were made based on H&E-stained slides of recurrent samples and read by three experienced pathologists (Z.M., H.K., and M.N.). The pathologists were blinded to clinical data and the patient group classification (RAI-R versus RAI-A), ensuring an unbiased evaluation of the findings. Histological growth patterns, including papillary and follicular patterns, along with the presence of tall cell and the LOP/LCC components, were recorded, and the proportion of each component was quantitatively assessed relative to the overall tumor size. The presence of tall cells, characterized by obtaining the tumor cell height at least thrice, was determined based on the 5th edition of the World Health Organization (WHO) classification [28]. LOP/LCC were described as a group of cancer cells exhibiting micropapillary and hobnail structure [17, 18, 29]. In addition, this study considered following structures as LOP/LCC components in the invasive front of PTC; solitary arrangement (defined as a loosely arranged solitary cell) and small nests (defined as loosely arranged small clusters without papillary or follicular arrangement or sheets of cells arranged in one or more regular rows). The invasive front was characterized as the boundary (< 0.1 cm) between the tumor tissue and the surrounding non-neoplastic thyroid tissue, lymph nodes or fatty connective tissue outside the thyroid capsule, where invasive growth was present [17]. When the LOP/LCC components were histologically identified in more than two foci in the invasive front of the tumor, the tumor was determined to be positive for this feature [18].

The mitotic count was determined as the number of mitoses per 2 mm² in areas of the tumor with the highest mitotic activity of tumor areas [28, 30], then dichotomized into 4 sets of two groups: mitosis count < 2 and ≥ 2, <3 and ≥ 3, <4 and ≥ 4, and < 5 and ≥ 5, which aligns with definitions of the 5th edition of the WHO classification for differentiated high-grade thyroid carcinoma [28, 31].

Clinical covariates

This study included clinical covariates, such as age at initial diagnosis, sex, primary tumor size, histological subtypes of primary PTC, and the Tumor-Node-Metastasis (TNM) staging at initial diagnosis, following previous studies assessing their association with RAI-R [6–8]. Age (grouped as < 55 and ≥ 55 years) and TNM staging were defined following the American Joint Committee on Cancer (AJCC) 8th Edition [32].

Statistical analyses

Continuous variables were summarized as medians and interquartile range (IQR) for non-normally distributed variables and compared using the Wilcoxon–Mann–Whitney test. Categorical variables were summarized as frequencies and percentages and compared using the chi-square or Fisher's tests. Logistic regression analysis was performed to estimate the odds ratios (OR) and 95% confidence interval (CI) of RAI-R in relation to $BRAF^{V600E}$ (irrespective of *TERT*-p mutation), *TERT*-p (irrespective of $BRAF^{V600E}$), Dmut, tall cell components, mitosis count, and Ki-67 LI. Analyses were performed using an unadjusted model and a multivariable model adjusted for age, sex, stage, papillary/follicular pattern, $BRAF^{V600E}$, *TERT*-p, tall cell component, mitosis count, and Ki-67 LI. For example, the association between mitotic count and RAI-R was adjusted for age, sex, stage, papillary/follicular pattern, $BRAF^{V600E}$, *TERT*-p, tall-cell components, and Ki-67 LI. *P*-values for trend in regression models were used to determine if increasing levels of the combination factors ($BRAF^{V600E}$/*TERT*-p, $BRAF^{V600E}$/Tall cell, $BRAF^{V600E}$/Mitosis, $BRAF^{V600E}$/Ki-67 LI, *TERT*-p/Ki-67 LI) were associated with a consistent increase in the odds of RAI-R. For example, the trend association between $BRAF^{V600E}$/*TERT*-p and RAI-R was assessed by assigning an ordinal number (1 to 3) to the mutation status, such

as wild-type, Smut, or Dmut, which were then treated as continuous variables in the regression models. Given the relatively small number of RAI-A group, Bootstrap resampling, with 500 iterations, was employed to assess the robustness of the regression models. Statistical significance was set at $p < 0.05$. All statistical analyses were performed using RStudio (Version 2023.6.0.421, RStudio Team, Boston, USA) [33].

Results

Clinical, pathological, and mutational characteristics of patients with PTC regarding RAI-R status

Of the 174 study participants, 156 and 18 cases were analyzed from recurrence of lymph nodes and thyroid beds, respectively. Table 1 presents the clinicopathological and mutational characteristics of PTC based on RAI-R status. Of the 174 study participants, 138 (79.3%) were women, and 135 (77.6%) were RAI-R cases. The ratio of

Table 1 Characteristics of patients with papillary thyroid carcinoma (PTC) in terms of RAI status

	Total	**RAI-*R***	**RAI-A**	
Factors	***n*** **= 174 (%)**	***n*** **= 135 (%)**	***n*** **= 39 (%)**	***P*-value**
Age (≥ 55 years)	53 (30.5)	48 (35.6)	5 (12.8)	**0.012**[a]
Sex (women)	138 (79.3)	106 (78.5)	32 (82.1)	0.798 [a]
Tumor size (mm), median (IQR)	20.0 (20)	20.0 (20)	15.0 (10)	0.230 [b]
Not available	16	12	4	
pT				0.089 [c]
T1	85 (48.9)	62 (45.9)	23 (59.0)	
T2	28 (16.1)	23 (17.0)	5 (12.8)	
T3a	3 (1.7)	2 (1.5)	1 (2.6)	
T3b	20 (11.5)	13 (9.6)	7 (17.9)	
T4	28 (16.1)	26 (19.3)	2 (5.1)	
Not available	10 (5.7)	9 (6.7)	1 (2.6)	
pN				0.505 [c]
N0	42 (24.1)	35 (25.9)	7 (17.9)	
N1a	21 (12.1)	15 (11.1)	6 (15.4)	
N1b	111 (63.8)	85 (63.0)	26 (66.7)	
Distant metastasis	7 (4.0)	7 (5.2)	0 (0)	0.351 [c]
pStage II + III + IV	53 (30.5)	48 (35.6)	5 (12.8)	**0.012**[a]
Histological subtype of primary tumors*				0.487 [c]
Classical PTC	167 (96.0)	128 (94.8)	39 (100)	
Follicular PTC	6 (3.4)	6 (4.5)	0 (0)	
Tall cell PTC	1 (0.6)	1 (0.7)	0 (0)	
Histological components of recurrent tumors**				
Papillary > follicular	121 (69.5)	93 (68.9)	28 (71.8)	0.881 [a]
Tall cell > 5%	25 (14.4)	24 (17.8)	1 (2.6)	**0.033**[a]
LOP/LCC > 1%	16 (9.2)	16 (11.9)	0 (0)	**0.024**[c]
micropapillary structures	7 (43.7)	7 (43.7)	0 (0)	
hobnail structures	4 (25.0)	4 (25.0)	0 (0)	
solitary arrangements	8 (50.0)	8 (50.0)	0 (0)	
small nests	14 (87.5)	14 (87.5)	0 (0)	
Mitosis count per 2 mm^2				
≥ 2	48 (27.6)	44 (32.6)	4 (10.3)	**0.011**[a]
≥ 3	24 (13.8)	23 (17.0)	1 (2.6)	**0.041**[a]
≥ 4	13 (7.5)	12 (8.9)	1 (2.6)	0.302 [c]
≥ 5	9 (5.2)	8 (5.9)	1 (2.6)	0.686 [c]
Ki-67 LI > 3%	73 (42.0)	61 (45.2)	12 (30.8)	0.155 [a]
Presence of mutation				
$BRAF^{V600E}$	139 (79.9)	115 (85.2)	24 (61.5)	**0.003**[a]
TERT-p	37 (21.3)	35 (25.9)	2 (5.1)	**0.010**[a]
Double	36 (20.7)	34 (25.2)	2 (5.1)	**0.001**[a]

[a] Chi-square test; [b] Wilcoxon test; [c] Fisher's exact test; RAI, radioactive iodine; RAI-R, RAI-refractory; RAI-A, RAI-avid; IQR, interquartile range; LOP/LCC, loss of polarity/loss of cell cohesiveness *TERT*-p: *TERT* promoter mutation; $BRAF^{V600E}$: irrespective of *TERT*-p; *TERT*-p, irrespective of $BRAF^{V600E}$; Ki-67 LI, labeling index. *Histological subtypes of primary tumors were based only on reports (from 2006 to 2022) but not on hematoxylin and eosin (H&E) stains due to unavailable primary samples. **Histological components of recurrent tumors were described based on H&E stains using the 5th edition of the World Health Organization (WHO) classification

age ≥ 55 was significantly larger in RAI-R than in RAI-A patients (35.6% vs. 12.8%, $p = 0.012$). The percentage of pStage II + III + IV disease was higher in RAI-R than in the RAI-A patients (35.6% vs. 12.8%, $p = 0.012$). Regarding the histological components in recurrent lesions, LOP/LCC components were exclusively present in the RAI-R group, and the rate of cases with > 5% tall cells in the entire tumor component was significantly higher in the RAI-R group than in the RAI-A group (17.8% vs. 2.6%, $p = 0.033$). The mitotic count was dichotomized into two groups: mitosis count < 2 and ≥ 2 based on the receiver operating characteristic curve analysis (Fig. 1). Specifically, the optimal cut-off value of mitosis count for RAI-R prediction was 1.5 (round up to 2), resulting in an

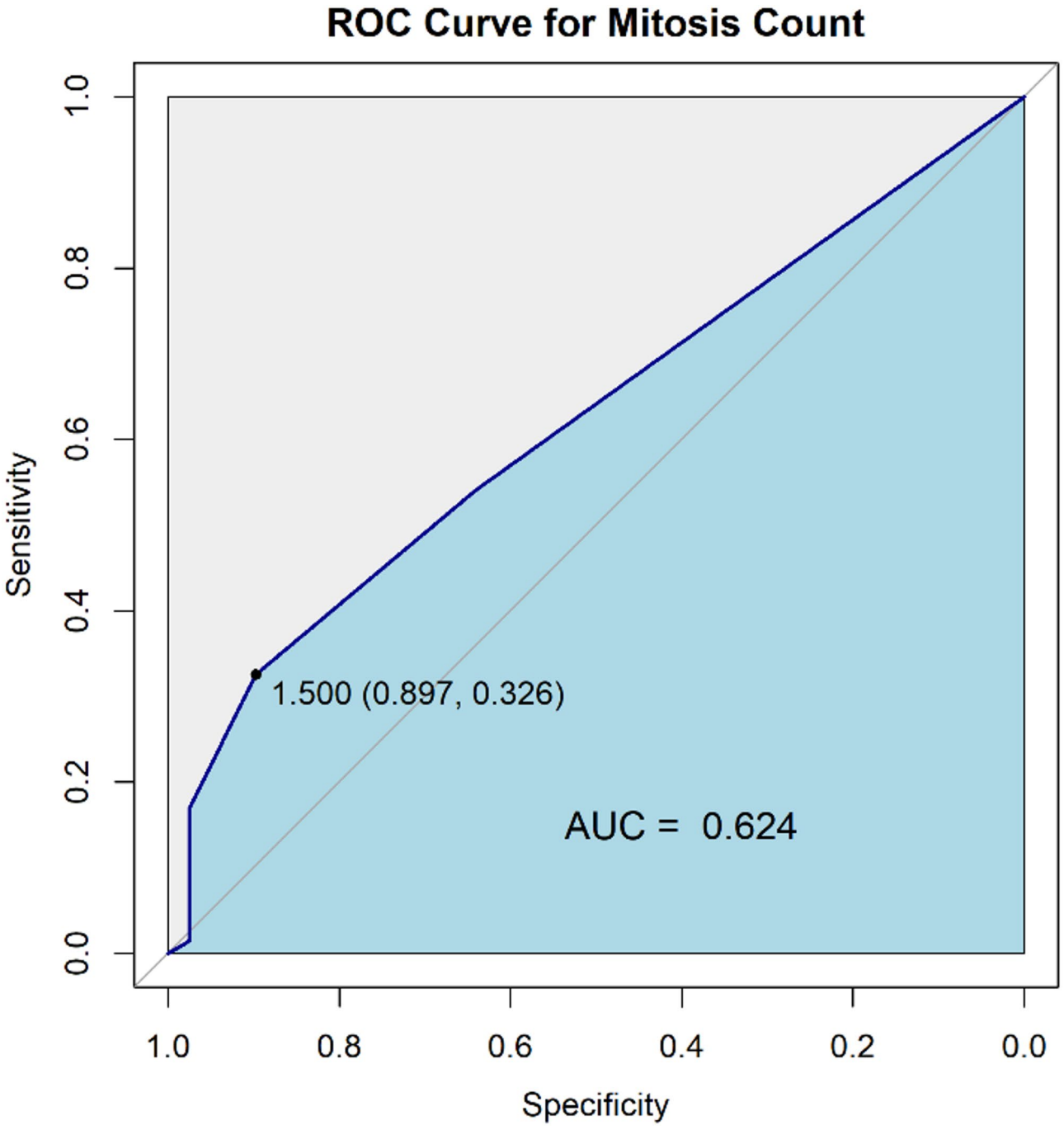

Fig. 1 Receiver operating characteristic (ROC) curve analysis of mitosis count to predict radioactive iodine-refractory (RAI-R) cases. The optimal mitosis count was 1.5 to predict RAI-R with an area under the ROC curve (AUC) of 0.624, 95% confidence interval of 0.542 – 0.707, sensitivity of 32.6%, specificity of 89.7%, and Youden index of 0.223

accuracy of 0.624 (95% CI: 0.542 – 0.707), sensitivity of 32.6%, and specificity of 89.7%. A high mitotic count (≥ 2 per 2 mm^2) was more frequently observed in the RAI-R than in the RAI-A group (32.6% vs. 10.3%, $p = 0.011$). Although the proportion of cases with a Ki-67 LI > 3% was higher in the RAI-R group than in the RAI-A group (45.2% vs. 30.8%, $p = 0.155$), the difference was not statistically significant. Regarding the presence of mutations, both $BRAF^{V600E}$ and *TERT*-p mutations were significantly more frequent in the RAI-R than in the RAI-A groups ($BRAF^{V600E}$: 85.2% vs. 61.5%, $p = 0.003$; *TERT*-p mutation: 25.9% vs. 5.1%, $p = 0.010$; Dmut: 25.2% vs. 5.1%, $p = 0.001$).

In this study, LOP/LCC components such as micropapillary structures were observed in seven of 16 cases, hobnail structures in four of 16 cases, solitary arrangements in eight of 16 cases, and small nests in 14 of 16 cases at the invasive front of the tumors. Representative images are shown in Fig. 2. In most cases, LOP/LCC components displayed multiple features simultaneously.

Association between mutations/pathological features and RAI-R

Table 2 shows the association of each factor, including $BRAF^{V600E}$, *TERT*-p, tall cell component, mitosis count, and Ki-67 LI, with RAI-R. In the unadjusted model, the OR (95% CI) was 3.59 (1.61–8.01), comparing $BRAF^{V600E}$ mutation vs. *BRAF* wild-type. This association remained statistically significant in the multivariate analysis. For *TERT*-p mutation, although the association with RAI-R was significant in the unadjusted model (OR: 6.47, 95% CI: 1.48–28.3), it was not significant in the multivariable model. Concerning mutation status, such as wild-type, Smut, and Dmut, both models revealed a significant stepwise increase in the association with RAI-R. The presence of tall cells > 5% and mitosis count ≥ 2 per 2 mm^2 were significantly associated with RAI-R in the unadjusted model but became marginally associated with RAI-R in multivariate models. Ki-67 LI > 3% were not significantly associated with RAI-R in both unadjusted and multivariable models. These associations were confirmed and remained stable in Bootstrap resampling models (Supplementary Table 1).

Association between combined factors of mutations/pathological features and RAI-R

Table 3 shows the association between combined mutations and pathological features, such as $BRAF^{V600E}$/*TERT*-p mutation and tall cell component/mitosis count/Ki-67 LI, and RAI-R. All six combinations were significantly associated with RAI-R. The association between combined mutations and pathological features with RAI-R using logistic regression analysis is summarized in Table 4. Among the combinations, because of the absence of combinations of *TERT*-p mutation and mitosis count ≥ 2/tall cell component in the RAI-A group, we excluded these two combinations in the logistic regression analysis. Multivariable logistic regression models indicated that likelihood of RAI-R was significantly associated with combinations of $BRAF^{V600E}$ and/or Tall cell > 5%, $BRAF^{V600E}$ and/or Mitosis ≥ 2/2mm^2. For example, the OR for RAI-R, comparing the presence of single or both $BRAF^{V600E}$ and Tall cell > 5% with none of them, was 2.94 (95%CI: 1.22 – 7.13), and 12.2 (95%CI: 1.35 – 110), respectively (*P*-value for trend = 0.003). Bootstrap resampling also yielded similar results (Supplementary Table 1).

To compare the impacts of combinations of Dmut, Smut, and no mutation with tall cell component, mitosis count, and Ki-67 LI on RAI-R, we performed additional analyses, as shown in Supplementary Tables 2 and 3. All combinations of Dmut exhibited higher proportions in the RAI-R group (Supplementary Table 2). Due to the absence of combined Dmut with tall cell/mitosis count in the RAI-A group, only Dmut/Ki-67 LI was analyzed in the logistic regression analysis (Supplementary Table 3). In unadjusted models, RAI-R was significantly associated with Smut, Dmut (irrespective of Ki-67 LI), with higher odds of RAI-R in combinations of Dmut. In multivariable models, Smut/Ki-67 LI became not significantly associated with RAI-R, whereas Dmut/Ki-67 LI remained associated considerably with RAI-R.

Discussion

This study identified several clinicopathological and molecular factors that were significantly associated with RAI-R PTC compared to RAI-A cases. Particularly, we observed a higher prevalence of age ≥ 55 years, pStage II + III + IV, tall cell components > 5%, LOP/LCC > 1%, mitosis count ≥ 2 per 2 mm^2, and the presence of $BRAF^{V600E}$/*TERT*-p mutations in patients with RAI-R PTC. Multivariate logistic regression analysis confirmed a significant association between $BRAF^{V600E}$ (irrespective of *TERT*-p mutation) and combined mutation status (Smut: $BRAF^{V600E}$ or *TERT*-p mutation alone and Dmut: coexistence of $BRAF^{V600E}$ and *TERT*-p mutations) with RAI-R. The results showed that the odds ratio for RAI-R was higher in Dmut compared to Smut, indicating that this combination was strongly associated with RAI-R (Table 2).

Histopathology remains a critical factor in predicting the prognosis of thyroid cancer. Aggressive histological subtypes of PTC, such as tall cell, hobnail, solid/trabecular, columnar cell, and diffuse sclerosing subtypes, have consistently been linked to worse outcomes, including higher rates of recurrence, distant metastases, and reduced overall survival [4, 34–36]. Additionally, previous studies have demonstrated a relationship between these aggressive histological subtypes and RAI-R [6, 8, 37,

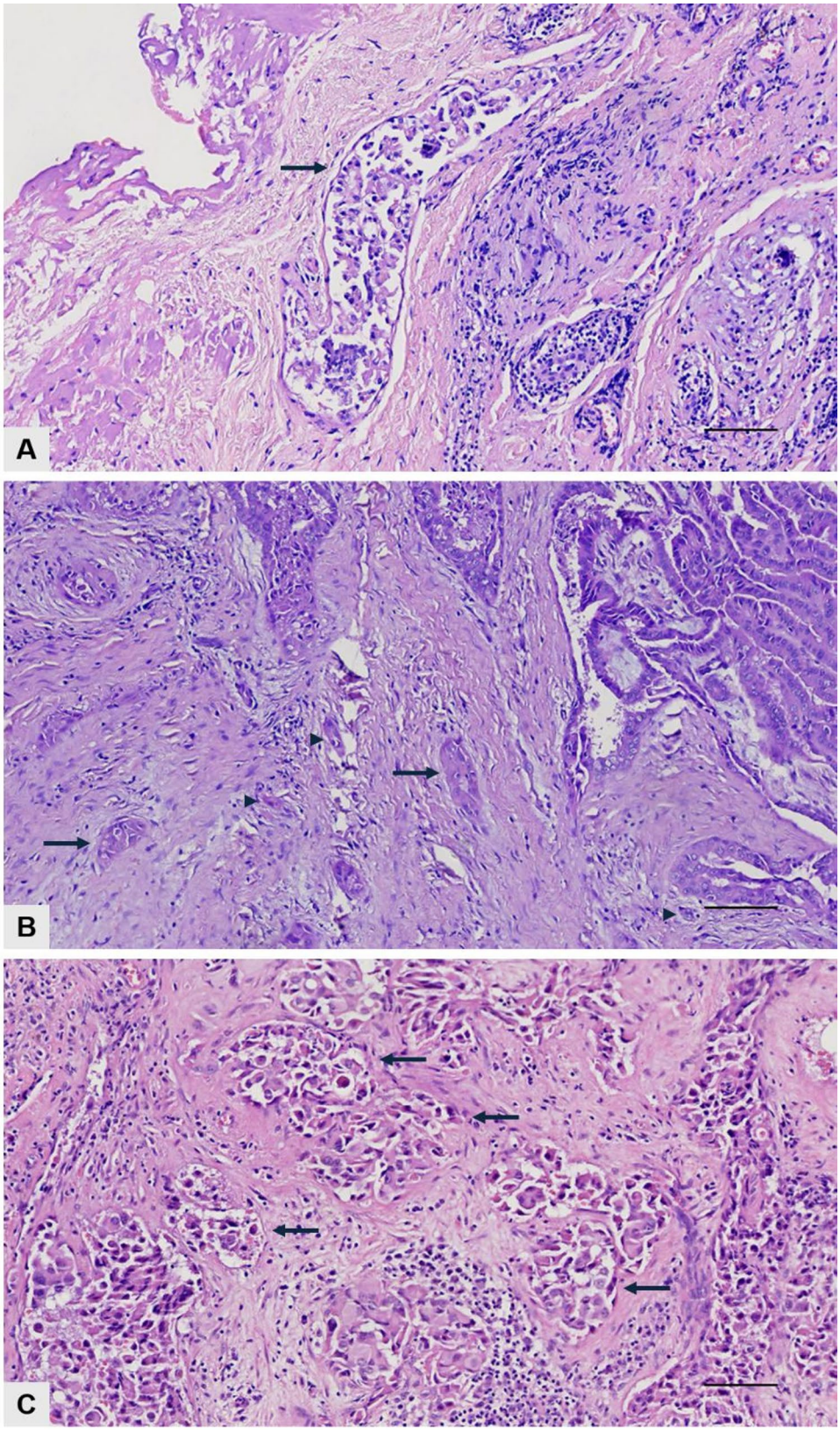

Fig. 2 Histological finding of loss of polarity/loss of cell cohesiveness (LOP/LCC) component in the invasive front area (hematoxylin–eosin). Scale bars indicated 120 μm. **A**, micropapillary **B**, solitary (arrowheads) and small nests (arrows). **C**, small nests

Table 2 ORs with 95% CIs of respective factors for RAI-R PTC

	Unadjusted		Multivariable	
Factors	**OR (95% CI)**	***P*-value**	**OR (95% CI)**	***P*-value**
BRAF^{V600E} mutation	3.59 (1.61 – 8.01)	**0.002**	2.67 (1.12 – 6.38)	**0.027**
TERT-p mutation	6.47 (1.48 – 28.3)	**0.013**	2.61 (0.52 – 13.0)	0.242
BRAF^{V600E}/*TERT*-p*				
Wildtype	1		1	
Single mutation	2.94 (1.29 – 6.71)	**0.010**	2.75 (1.14 – 6.62)	**0.024**
Double mutation	13.4 (2.77 – 65.1)	**0.001**	6.64 (1.23 – 35.9)	**0.028**
P-value for trend	**< 0.001**		**0.007**	
Tall cell > 5%	8.22 (1.08 – 62.8)	**0.042**	6.51 (0.79 – 53.9)	0.082
Mitosis ≥ 2/2 mm^2	4.23 (1.41 – 12.6)	**0.010**	2.92 (0.88 – 9.67)	0.079
Ki-67 LI > 3%	1.85 (0.87 – 3.97)	0.111	1.18 (0.49 – 2.86)	0.710

ORs, Odds ratios; CIs, confidence intervals; RAI-R, radioactive iodine-refractory; PTC, papillary thyroid carcinoma; *TERT*-p: *TERT* promoter mutation; *BRAF*^{V600E}: irrespective of *TERT*-p; *TERT*-p, irrespective of *BRAF*^{V600E}; Mutation status: *BRAF*^{V600E} /*TERT*-p; Single mutation: *BRAF*^{V600E} alone or *TERT*-p alone; Ki-67 LI: labeling index

Multivariable analysis included age, sex, stage, papillary/follicular pattern, *BRAF*^{V600E}, *TERT*-p, tall cell, mitosis, and Ki-67 LI. *Excluded *BRAF*^{V600E} and *TERT*-p, but included *BRAF*^{V600E}/*TERT*-p

Table 3 Statistical analyses of associations between combined mutation and pathological factors with PTC in terms of RAI status

	Total	RAI-*R*	RAI-A	
Combined factors	***n* = 174 (%)**	***n* = 135 (%)**	***n* = 39 (%)**	***P*-value**
BRAF^{V600E}/Tall cell > 5%				**0.001**[a]
none	33 (19.0)	18 (13.3)	15 (38.4)	
or	118 (67.8)	95 (70.4)	23 (59.0)	
and	23 (13.2)	22 (16.3)	1 (2.6)	
BRAF^{V600E}/Mitosis ≥ 2/2mm^2				**< 0.001**[a]
none	28 (16.1)	14 (10.4)	14 (35.9)	
or	105 (60.3)	83 (61.5)	22 (56.4)	
and	41 (23.6)	38 (28.1)	3 (7.7)	
BRAF^{V600E}/Ki-67 LI > 3%				**0.001**[b]
none	22 (12.6)	10 (7.4)	12 (30.8)	
or	92 (52.9)	74 (54.8)	18 (46.1)	
and	60 (34.5)	51 (37.8)	9 (23.1)	
TERT-p/Tall cell > 5%				**0.001**[b]
none	121 (69.5)	85 (63.0)	36 (92.3)	
or	44 (25.3)	41 (30.4)	3 (7.7)	
and	9 (5.2)	9 (6.6)	0 (0)	
TERT-p/Mitosis ≥ 2/2mm^2				**0.004**[a]
none	112 (64.4)	79 (58.5)	33 (84.6)	
or	39 (22.4)	33 (24.5)	6 (15.4)	
and	23 (13.2)	23 (17.0)	0 (0)	
TERT-p/Ki-67 LI > 3%				**0.024**[a]
none	91 (52.3)	65 (48.1)	26 (66.7)	
or	56 (32.2)	44 (32.6)	12 (30.8)	
and	27 (15.5)	26 (19.3)	1 (2.5)	

[a] Chi-square test; [b] Fisher's exact test; RAI-R, radioactive iodine-refractory; PTC, papillary thyroid carcinoma; RAI-A, radioactive iodine-avid; Ki-67 LI, labeling index; *TERT*-p, *TERT* promoter mutation; none, neither of the two factors; or, one of the two factors; and, a combination of the two factors

38]. Consistent with these previous findings, we observed a significantly higher level of tall cell components (> 5%) in patients with RAI-R PTC than in those with RAI-A PTC, supporting the notion that tall cell components, especially in conjunction with *BRAF*^{V600E}, are key predictors of RAI refractoriness. Deficiency in RAI uptake in the tall cell component can be explained by the impaired the sodium-iodide symporter (NIS) expression in these subtypes [39]. Wei et al. found that 73% of classical PTCs showed positive NIS expression, whereas NIS expression was only observed in 32% of tall cell PTCs [39].

Our study also explored the presence of LOP/LCC components, which have not been extensively studied in the context of RAI-R PTC. We found that LOP/LCC components were present in recurrent cancers in the RAI-R group but absent in the RAI-A group. Although

Table 4 ORs with 95% CIs of combined mutation and pathological factors for RAI-R PTC

	Unadjusted		Multivariable	
Combined factors	**OR (95% CI)**	***P*-value**	**OR (95% CI)**	***P*-value**
BRAF^{V600E}/Tall cell > 5% [a]				
none	1		1	
or	3.44 (1.51 – 7.84)	**0.003**	2.94 (1.22 – 7.13)	**0.017**
and	18.3 (2.21 – 152)	**0.007**	12.2 (1.35 – 110)	**0.026**
P-value for trend	**< 0.001**		**0.003**	
BRAF^{V600E}/Mitosis ≥ 2/2mm^2 [b]				
none	1		1	
or	3.77 (1.57 – 9.07)	**0.003**	3.44 (1.35 – 8.79)	**0.010**
and	12.7 (3.16 – 50.8)	**< 0.001**	5.86 (1.26 – 27.2)	**0.024**
P-value for trend	**< 0.001**		**0.007**	
BRAF^{V600E}/Ki-67 LI > 3% [c]				
none	1		1	
or	4.93 (1.84 – 13.2)	**0.001**	4.74 (1.63 – 13.8)	**0.004**
and	6.80 (2.27 – 20.4)	**< 0.001**	3.29 (0.94 – 11.5)	0.061
P-value for trend	**0.002**		0.080	
TERT-p/Ki-67 LI > 3% [d]				
none	1		1	
or	1.47 (0.67 – 3.21)	0.338	1.16 (0.49 – 2.76)	0.733
and	10.4 (1.34 – 80.6)	**0.025**	4.17 (0.47 – 36.7)	0.198
P-value for trend	**0.011**		0.252	

ORs, Odds ratios; CIs, confidence intervals; PTC, papillary thyroid carcinoma; RAI-R, radioactive iodine-refractory; *TERT*-p: *TERT* promoter mutation; *BRAF*^{V600E}: irrespective of *TERT*-p; *TERT*-p, irrespective of *BRAF*^{V600E}; none, neither of the two factors; or, one of the two factors; and, a combination of the two factors; Ki-67 LI, labeling index

Multivariable analysis included age, sex, stage, papillary/follicular pattern, *BRAF*^{V600E}, *TERT*-p, tall cell, mitosis, and Ki-67 LI. In multivariable analysis: [a]Excluded *BRAF*^{V600E} and tall cell, but included *BRAF*^{V600E}/Tall cell; [b]Excluded *BRAF*^{V600E} and mitosis, but included *BRAF*^{V600E}/Mitosis; [c]Excluded *BRAF*^{V600E} and Ki-67 LI, but included *BRAF*^{V600E}/Ki-67 LI; [d]Excluded *TERT*-p and Ki-67 LI, but included *TERT*-p/Ki-67 LI.

the absence of these components in RAI-A cases prevented us from fully assessing their independent predictive role, the presence of LOP/LCC components in RAI-R tumors suggests that these histological features may be important for determining the risk of RAI-R. However, to our knowledge, no study has investigated the association between RAI-R and LOP/LCC. We suggest that the LOP/LCC components may be histopathological markers of RAI refractoriness and should be further investigated in future studies.

In addition to histological factors, we examined mitotic counts and Ki-67 LI in relation to RAI-R. According to the 5th edition of the WHO classification, a mitotic count of at least 3 and 5 per 2 mm^2 is required to diagnose poorly and high-grade differentiated thyroid carcinoma, respectively [28]. Although our univariable analysis showed a significant association between mitosis count ≥ 2 per 2 mm^2 and RAI-R, this association became marginal in the multivariable model. This suggests that mitosis count alone may not be a strong predictor but could be relevant when combined with genetic factors such as *BRAF*^{V600E} and/or *TERT* -p mutations. This has also been reported in previous studies, suggesting a synergistic effect [40, 41]. Regarding Ki-67 LI, our analysis did not reveal a significant association with RAI-R, even when combined with other markers. This suggests that a Ki-67 LI > 3% may not be a useful predictor of RAI-R and may not have a synergistic effect at a cut-off of > 3% with these mutations on RAI-R.

The molecular landscape also plays a crucial role in predicting RAI-R. The prevalence of *BRAF*^{V600E} in PTC varies geographically and ranges from 25 to 89% [42]. In our study, *BRAF*^{V600E} was found in 85.2% of RAI-R cases, consistent with a previous study from Vietnam [38]. *TERT*-p mutations, which have been associated with more aggressive tumor behavior, were also more common in patients with RAI-R PTC (25.9%) than in those with RAI-A PTC (5.1%). Importantly, most *TERT*-p mutation-positive cases also harbored *BRAF*^{V600E} mutations (97.3%). Our multivariate analysis demonstrated that Dmut had a stronger association with RAI-R than Smut (Table 2). This finding aligns with previous studies suggesting that the co-occurrence of *BRAF*^{V600E} and *TERT*-p mutations is a stronger predictor of RAI-R than either mutation alone [9, 10]. This study is also the first to characterize *TERT*-p mutations (C228T and C250T) and their combination with *BRAF*^{V600E} in Vietnamese papillary thyroid carcinoma patients. The incidence of *TERT*-p in our study was 21.3%, which is higher than that reported in previous studies (9.8–10.6%) of PTC patients [43, 44]. A possible explanation for this higher rate is that all the cases in our study involved recurrent PTC

patients, while *TERT*-p was known to be associated with persistent or recurrent disease [43].

This study had several limitations. First, the initial surgeries were conducted at multiple institutions, which led to incomplete data regarding the primary tumors (e.g., tumor size and T stage) for some patients. Second, mutations and histopathological features may change from primary to recurrent tumors. However, we were not able to examine these potential changes, if any, due to the unavailability of primary tumor samples. Future studies should address this gap by including paired primary-recurrent tumor samples to investigate the evolutionary mechanisms underlying RAI-R progression. Third, the imbalance between RAI-A ($n = 39$) and RAI-R ($n = 135$) groups might have compromised the robustness of multivariate analyses. However, our additional Bootstrap resample analyses confirmed that our findings are stably significant. Fourth, given the limitation of the cross-sectional study design, the present findings may not imply a causal relationship. Future research should incorporate longitudinal follow-up of large cohorts to validate our findings. Furthermore, investigation for other genetic changes, such as *RAS*, *RET/PTC* rearrangements, *NTRK* fusion, or *ALK* fusion remains to be elucidated for a more comprehensive understanding of molecular mechanisms with RAI-R. Prospective studies should focus on LOP/LCC components and mechanistic studies on NIS expression, whereas the role of mitotic count and Ki-67 in combination with genetic factors warrants further exploration.

Conclusion

Our study demonstrates that $BRAF^{V600E}$ and Dmut are independent predictors of RAI-R in Vietnamese patients with recurrent PTC. Additionally, although the presence of LOP/LCC components in RAI-R tumors suggests its potential role as a predictor of RAI-R PTC, further investigation with larger datasets is required to confirm this finding. The association between Dmut and RAI-R was stronger than that between Smut and RAI refractoriness, reinforcing the importance of considering coexisting mutations in predicting RAI refractoriness. Future studies should focus on elucidating the role of mitotic count and LOP/LCC components in RAI-R PTC.

Abbreviations

PTC	Papillary thyroid carcinomas
RAI	Radioactive iodine
RAI-A	RAI-avid
RAI-R	Radioactive iodine-refractory
TERT-p	Telomere Reverse Transcriptase promoter
LOP/LCC	Loss of polarity/loss of cell cohesiveness
EMT	Epithelial-mesenchymal transition
Ki-67 LI	Ki-67 labeling index
FFPE	Formalin-fixed paraffin-embedded
H&E	Hematoxylin and eosin
Smut	Single mutant
Dmut	Double mutant
WHO	World Health Organization
TNM	Tumor-Node-Metastasis
AJCC	American Joint Committee on Cancer
IQR	Interquartile range
OR	Odds ratio
95% CI	95% confidence interval
NIS	Sodium-iodide symporter

Supplementary Information

The online version contains supplementary material available at https://doi.org/10.1186/s12902-025-01954-9.

Supplementary Material 1

Acknowledgements

We thank the 108 Central Military Hospital, especially the Department of Nuclear Medicine, for the treatment and follow-up of patients, the Department of Pathology for preparing patient samples, and the Department of Thorax Surgery for detailed surgery reports of patients.

Author contributions

MN supervised this study. MN, NHL, and TNN designed the study. TNN, TMHN, VPTN, MSL, and TPN collected data. TNN, ZM, KM, YM, VPTN, KT, TNAN, and YS performed pathological and molecular analyses. ZM, HK, and MN interpreted and confirmed the results of the pathological and molecular analyses. VDH and TNN performed statistical analyses. NHL provided clinical conceptualization and advice. TNN, ZM, VDH, and MN wrote the manuscript. MN revised and edited the manuscript. The authors have read and approved the final version of the manuscript.

Funding

This work was funded by the Atomic Bomb Disease Institute, Nagasaki University and the Program of the Network-Type Joint Usage/Research Center for Radiation Disaster Medical Science.

Data availability

The datasets generated and analyzed in this study are available from the corresponding author on reasonable request.

Declarations

Ethics approval and consent to participate

This study was conducted in accordance with the principles of the Declaration of Helsinki. The study protocol was approved by the Institutional Review Board of the 108 Military Central Hospital (5199/GCN-BV) and the Institutional Ethical Committee for Medical Research at Nagasaki University (#15062617-6). Informed consent was obtained from all participants.

Consent to publish

Not applicable.

Competing interests

The authors declare no competing interests.

Clinical trial number

Not applicable.

Author details

[1]Department of Tumor and Diagnostic Pathology, Atomic Bomb Disease Institute, Graduate School of Biomedical Sciences, Nagasaki University, 1-12-4 Sakamoto, Nagasaki 852-8523, Japan
[2]Department of Fundamental Medicine, Al-Farabi Kazakh National University, Almaty 050040, Kazakhstan
[3]Medical Oncology Clinical Trial Unit Fiona Stanley Hospital, 11 Robin Warren Drive, Murdoch, WA 6150, Australia
[4]Department of Nuclear Medicine, 108 Military Central Hospital, Ha Noi, Vietnam
[5]Department of Pathology, 108 Military Central Hospital, Ha Noi, Vietnam

Received: 7 February 2025 / Accepted: 8 May 2025
Published online: 20 May 2025

References

1. Megwalu UC, Moon PK. Thyroid cancer incidence and mortality trends in the united States: 2000–2018. Thyroid. 2022;32:560–70. https://doi.org/10.1089/thy.2021.0662.
2. Schlumberger MJ. Papillary and follicular thyroid carcinoma. N Engl J Med. 1998;338:297–306. https://doi.org/10.1056/NEJM199801293380506.
3. Durante C, Haddy N, Baudin E, Leboulleux S, Hartl D, Travagli JP, Caillou B, Ricard M, Lumbroso JD, De Vathaire F, et al. Long-term outcome of 444 patients with distant metastases from papillary and follicular thyroid carcinoma: benefits and limits of radioiodine therapy. J Clin Endocrinol Metab. 2006;91:2892–9. https://doi.org/10.1210/jc.2005-2838.
4. Haugen BR, Alexander EK, Bible KC, Doherty GM, Mandel SJ, Nikiforov YE, Pacini F, Randolph GW, Sawka AM, Schlumberger M, et al. 2015 American thyroid association management guidelines for adult patients with thyroid nodules and differentiated thyroid cancer: the American thyroid association guidelines task force on thyroid nodules and differentiated thyroid cancer. Thyroid. 2016;26:1–133. https://doi.org/10.1089/thy.2015.0020.
5. Filetti S, Durante C, Hartl DM, Leboulleux S, Locati LD, Newbold K, Papotti MG, Berruti A. clinicalguidelines@esmo.org EGCEa. ESMO clinical practice guideline update on the use of systemic therapy in advanced thyroid cancer. Ann Oncol. 2022;33:674–84. https://doi.org/10.1016/j.annonc.2022.04.009.
6. Liu W, Jiang B, Xue J, Liu R, Wei Y, Li P. Clinicopathological features of differentiated thyroid carcinoma as predictors of the effects of radioactive iodine therapy. Ann Diagn Pathol. 2024;69:152243. https://doi.org/10.1016/j.anndiagpath.2023.152243.
7. Meng C, Song J, Long W, Mu Z, Sun Y, Liang J, Lin Y. A user-friendly nomogram for predicting radioiodine refractory differentiated thyroid cancer. Front Endocrinol (Lausanne). 2023;14:1109439. https://doi.org/10.3389/fendo.2023.1109439.
8. Luo Y, Jiang H, Xu W, Wang X, Ma B, Liao T, Wang Y. Clinical, pathological, and molecular characteristics correlating to the occurrence of radioiodine refractory differentiated thyroid carcinoma: a systematic review and meta-analysis. Front Oncol. 2020;10:549882. https://doi.org/10.3389/fonc.2020.549882.
9. Liu J, Liu R, Shen X, Zhu G, Li B, Xing M. The genetic duet of BRAF V600E and TERT promoter mutations robustly predicts loss of radioiodine avidity in recurrent papillary thyroid cancer. J Nucl Med. 2020;61:177–82. https://doi.org/10.2967/jnumed.119.227652.
10. Cao J, Zhu X, Sun Y, Li X, Yun C, Zhang W. The genetic duet of BRAF V600E and TERT promoter mutations predicts the poor curative effect of radioiodine therapy in papillary thyroid cancer. Eur J Nucl Med Mol Imaging. 2022;49:3470–81. https://doi.org/10.1007/s00259-022-05820-x.
11. Soe MH, Chiang JM, Flavell RR, Khanafshar E, Mendoza L, Kang H, Liu C. Non-iodine-avid disease is highly prevalent in distant metastatic differentiated thyroid cancer with papillary histology. J Clin Endocrinol Metab. 2022;107:e3206–16. https://doi.org/10.1210/clinem/dgac305.
12. Huang S, Qi M, Tian T, Dai H, Tang Y, Huang R. Positive BRAFV600E mutation of primary tumor influences radioiodine avidity but not prognosis of papillary thyroid cancer with lung metastases. Front Endocrinol (Lausanne). 2022;13:959089. https://doi.org/10.3389/fendo.2022.959089.
13. Chai J, Zhang R, Zheng W, Zhang G, Jia Q, Tan J, Meng Z, Wang R. Predictive value of clinical and pathological characteristics for metastatic radioactive iodine-refractory differentiated thyroid carcinoma: a 16-year retrospective study. Front Endocrinol (Lausanne). 2022;13:930180. https://doi.org/10.3389/fendo.2022.930180.
14. Anekpuritanang T, Uataya M, Claimon A, Laokulrath N, Pongsapich W, Pithuksurachai P. The association between radioiodine refractory in papillary thyroid carcinoma, sodium/iodide symporter expression, and BRAF (V600E) mutation. Onco Targets Ther. 2021;14:3959–69. https://doi.org/10.2147/OTT.S308910.
15. Rossi ED, Pantanowitz L. Focal tall cell change in papillary thyroid carcinoma: lessons learned from practices adopting rigid criteria (Height to width ratio of 3). Endocr Pathol. 2024;35:80–1. https://doi.org/10.1007/s12022-024-09801-8.
16. Bongers PJ, Kluijfhout WP, Verzijl R, Lustgarten M, Vermeer M, Goldstein DP, Devon K, Rotstein LE, Asa SL, Brierley JD, et al. Papillary thyroid cancers with focal tall cell change are as aggressive as tall cell variants and should not be considered as low-risk disease. Ann Surg Oncol. 2019;26:2533–9. https://doi.org/10.1245/s10434-019-07444-2.
17. Liu Z, Kakudo K, Bai Y, Li Y, Ozaki T, Miyauchi A, Taniguchi E, Mori I. Loss of cellular polarity/cohesiveness in the invasive front of papillary thyroid carcinoma, a novel predictor for lymph node metastasis; possible morphological indicator of epithelial mesenchymal transition. J Clin Pathol. 2011;64:325–9. https://doi.org/10.1136/jcp.2010.083956.
18. Kakudo K, Tang W, Ito Y, Mori I, Nakamura Y, Miyauchi A. Papillary carcinoma of the thyroid in Japan: subclassification of common type and identification of low risk group. J Clin Pathol. 2004;57:1041–6. https://doi.org/10.1136/jcp.2004.017889.
19. Lindfors H, Ihre Lundgren C, Zedenius J, Juhlin CC, Shabo I. The clinical significance of lymph node ratio and Ki-67 expression in papillary thyroid cancer. World J Surg. 2021;45:2155–64. https://doi.org/10.1007/s00268-021-06070-y.
20. Ito Y, Miyauchi A, Kakudo K, Hirokawa M, Kobayashi K, Miya A. Prognostic significance of ki-67 labeling index in papillary thyroid carcinoma. World J Surg. 2010;34:3015–21. https://doi.org/10.1007/s00268-010-0746-3.
21. Metovic J, Cabutti F, Osella-Abate S, Orlando G, Tampieri C, Napoli F, Maletta F, Daniele L, Volante M, Papotti M. Clinical and pathological features and gene expression profiles of clinically aggressive papillary thyroid carcinomas. Endocr Pathol. 2023;34:298–310. https://doi.org/10.1007/s12022-023-09769-x.
22. Coca-Pelaz A, Rodrigo JP, Shah JP, Nixon IJ, Hartl DM, Robbins KT, Kowalski LP, Makitie AA, Hamoir M, Lopez F, et al. Recurrent differentiated thyroid cancer: the current treatment options. Cancers (Basel). 2023;15. https://doi.org/10.3390/cancers15102692.
23. Mazzaferri EL, Jhiang SM. Long-term impact of initial surgical and medical therapy on papillary and follicular thyroid cancer. Am J Med. 1994;97:418–28. https://doi.org/10.1016/0002-9343(94)90321-2.
24. Otsubo C, Mussazhanova Z, Kurohama H, Shalgimbayeva G, Ueki N, Matsuoka Y, Madiyeva M, Sato S, Yamashita H, Nakashima M. A new indicator to differentiate thyroid follicular inclusions in cervical lymph nodes from patients with thyroid cancer. Int J Mol Sci. 2022;24. https://doi.org/10.3390/ijms24010490.
25. Nakao T, Matsuse M, Saenko V, Rogounovitch T, Tanaka A, Suzuki K, Higuchi M, Sasai H, Sano T, Hirokawa M, et al. Preoperative detection of the TERT promoter mutations in papillary thyroid carcinomas. Clin Endocrinol (Oxf). 2021;95:790–9. https://doi.org/10.1111/cen.14567.
26. Tanaka A, Matsuse M, Saenko V, Nakao T, Yamanouchi K, Sakimura C, Yano H, Nishihara E, Hirokawa M, Suzuki K, et al. TERT mRNA expression as a novel prognostic marker in papillary thyroid carcinomas. Thyroid. 2019;29:1105–14. https://doi.org/10.1089/thy.2018.0695.
27. Hirokawa M, Matsuda K, Kudo T, Higuchi M, Suzuki A, Takada N, Nakashima M, Miyauchi A. Cribriform-morular variant of papillary thyroid carcinoma shows high Ki-67 labeling indices, despite its excellent prognosis. Pathobiology. 2019;86:248–53. https://doi.org/10.1159/000501097.
28. Baloch ZW, Asa SL, Barletta JA, Ghossein RA, Juhlin CC, Jung CK, LiVolsi VA, Papotti MG, Sobrinho-Simoes M, Tallini G, et al. Overview of the 2022 WHO classification of thyroid neoplasms. Endocr Pathol. 2022;33:27–63. https://doi.org/10.1007/s12022-022-09707-3.
29. Bai Y, Kakudo K, Nakamura M, Ozaki T, Li Y, Liu Z, Mori I, Miyauchi A, Zhou G. Loss of cellular polarity/cohesiveness in the invasive front of papillary thyroid carcinoma and Periostin expression. Cancer Lett. 2009;281:188–95. https://doi.org/10.1016/j.canlet.2009.02.043.
30. Cree IA, Tan PH, Travis WD, Wesseling P, Yagi Y, White VA, Lokuhetty D, Scolyer RA. Counting mitoses: SI(ze) matters! Mod Pathol. 2021;34:1651–7. https://doi.org/10.1038/s41379-021-00825-7.
31. Christofer Juhlin C, Mete O, Baloch ZW. The 2022 WHO classification of thyroid tumors: novel concepts in nomenclature and grading. Endocr Relat Cancer. 2023;30. https://doi.org/10.1530/ERC-22-0293.
32. Tuttle RM, Haugen B, Perrier ND. Updated American joint committee on cancer/tumor-node-metastasis staging system for differentiated and anaplastic thyroid cancer (eighth edition): what changed and why? Thyroid. 2017;27:751–6; https://doi.org/10.1089/thy.2017.0102
33. Posit Team. RStudio: integrated development environment for R. 2023.
34. Pizzimenti C, Fiorentino V, Ieni A, Martini M, Tuccari G, Lentini M, Fadda G. Aggressive variants of follicular cell-derived thyroid carcinoma: an overview. Endocrine. 2022;78:1–12. https://doi.org/10.1007/s12020-022-03146-0.
35. Nath MC, Erickson LA. Aggressive variants of papillary thyroid carcinoma: hobnail, tall cell, columnar, and solid. Adv Anat Pathol. 2018;25:172–9. https://doi.org/10.1097/PAP.0000000000000184.
36. Baloch Z, LiVolsi VA, Tondon R. Aggressive variants of follicular cell derived thyroid carcinoma; the so called 'real thyroid carcinomas'. J Clin Pathol. 2013;66:733–43. https://doi.org/10.1136/jclinpath-2013-201626.

37. Nilsson JN, Siikanen J, Condello V, Jatta K, Saini R, Hedman C, Ihre Lundgren C, Juhlin CC. Iodine avidity in papillary and poorly differentiated thyroid cancer is predicted by immunohistochemical and molecular work-up. Eur Thyroid J. 2023;12. https://doi.org/10.1530/ETJ-23-0099.
38. Ha LN, Iravani A, Nhung NT, Hanh NTM, Hutomo F, Son MH. Relationship between clinicopathologic factors and FDG avidity in radioiodine-negative recurrent or metastatic differentiated thyroid carcinoma. Cancer Imaging. 2021;21:8. https://doi.org/10.1186/s40644-020-00378-z.
39. Wei S, Gao M, Zhao C, Pan Y, Li H, Li J, Li X. Low expression of sodium iodide symporter expression in aggressive variants of papillary thyroid carcinoma. Int J Clin Oncol. 2014;19:800–4. https://doi.org/10.1007/s10147-013-0620-z.
40. Kim MJ, Kim JK, Kim GJ, Kang SW, Lee J, Jeong JJ, Chung WY, Kim D, Nam KH. TERT promoter and BRAF V600E mutations in papillary thyroid cancer: A Single-Institution experience in Korea. Cancers (Basel). 2022;14. https://doi.org/10.3390/cancers14194928.
41. Xing M, Alzahrani AS, Carson KA, Viola D, Elisei R, Bendlova B, Yip L, Mian C, Vianello F, Tuttle RM, et al. Association between BRAF V600E mutation and mortality in patients with papillary thyroid cancer. JAMA. 2013;309:1493–501. https://doi.org/10.1001/jama.2013.3190.
42. Wei X, Wang X, Xiong J, Li C, Liao Y, Zhu Y, Mao J. Risk and prognostic factors for BRAF(V600E) mutations in papillary thyroid carcinoma. Biomed Res Int. 2022;2022:9959649. https://doi.org/10.1155/2022/9959649.
43. Yang J, Gong Y, Yan S, Chen H, Qin S, Gong R. Association between TERT promoter mutations and clinical behaviors in differentiated thyroid carcinoma: a systematic review and meta-analysis. Endocrine. 2020;67:44–57. https://doi.org/10.1007/s12020-019-02117-2.
44. Park J, Lee S, Kim K, Park H, Ki CS, Oh YL, Shin JH, Kim JS, Kim SW, Chung JH, et al. TERT promoter mutations and the 8th edition TNM classification in predicting the survival of thyroid cancer patients. Cancers (Basel). 2021;13. https://doi.org/10.3390/cancers13040648.

Publisher's note